Neuropharmacology 85 (2014) 451–460

Contents lists available at ScienceDirect

Neuropharmacology

journal homepage: www.elsevier.com/locate/neuropharm

Concurrent and robust regulation of feeding behaviors and metabolism by orexin neurons

Ayumu Inutsuka [a], Azusa Inui [a], Sawako Tabuchi [a], Tomomi Tsunematsu [a], Michael Lazarus [b], Akihiro Yamanaka [a, *]

[a] Department of Neuroscience II, Research Institute of Environmental Medicine, Nagoya University, Nagoya 464-8601, Japan
[b] International Institute for Integrative Sleep Medicine (WPI-IIIS), University of Tsukuba, Tsukuba 305-8575, Japan

ARTICLE INFO

Article history:
Received 22 April 2014
Received in revised form
6 June 2014
Accepted 11 June 2014
Available online 18 June 2014

Keywords:
Orexin
Hypothalamus
Pharmacogenetics
Feeding
Metabolism

ABSTRACT

Orexin neurons in the hypothalamus regulate energy homeostasis by coordinating various physiological responses. Past studies have shown the role of the orexin peptide itself; however, orexin neurons contain not only orexin but also other neurotransmitters such as glutamate and dynorphin. In this study, we examined the physiological role of orexin neurons in feeding behavior and metabolism by pharmacogenetic activation and chronic ablation. We generated novel *orexin-Cre* mice and utilized Cre-dependent adeno-associated virus vectors to express Gq-coupled modified GPCR, hM3Dq or diphtheria toxin fragment A in orexin neurons. By intraperitoneal injection of clozapine-N oxide in *orexin-Cre* mice expressing hM3Dq in orexin neurons, we could selectively manipulate the activity of orexin neurons. Pharmacogenetic stimulation of orexin neurons simultaneously increased locomotive activity, food intake, water intake and the respiratory exchange ratio (RER). Elevation of blood glucose levels and RER persisted even after locomotion and feeding behaviors returned to basal levels. Accordantly, 83% ablation of orexin neurons resulted in decreased food and water intake, while 70% ablation had almost no effect on these parameters. Our results indicate that orexin neurons play an integral role in regulation of both feeding behavior and metabolism. This regulation is so robust that greater than 80% of orexin neurons were ablated before significant changes in feeding behavior emerged.

1. Introduction

The neuropeptide orexin (hypocretin) has been known to be involved in feeding behavior since its early identification. In 1998, two groups independently identified this neuropeptide. One group named it "hypocretin" as they had found the peptide in the hypothalamus (De Lecea et al., 1998), and the other group named it "orexin" due to its putative role as a regulator of feeding behavior (Sakurai et al., 1998). Orexin is now known to regulate not only feeding but also various phenomena including arousal, addiction, and metabolism (Sakurai, 2007; Inutsuka and Yamanaka, 2013; De Lecea and Huerta, 2014). Although orexin neurons exist exclusively in the lateral hypothalamic area (LHA), they project their axons throughout the brain including the arcuate nucleus (Arc) where many regulators of feeding behaviors such as proopiomelanocortin and neuropeptide Y (NPY) neurons are present (Peyron et al., 1998; Nambu et al., 1999). Intracerebroventricular (ICV) injection of orexin induces feeding behavior (Sakurai et al., 1998) and water intake (Kunii et al., 1999) in rodents. In addition, injection of orexin-A into the rostral raphe pallidus produces a sustained increase in brown adipose tissue thermogenesis (Tupone et al., 2011).

Although the functions of orexin peptides have already been studied, the contribution of orexin neuronal activity to feeding behavior remains unclear. Narcolepsy is a sleep disorder characterized by primary disorganization of sleep/wakefulness cycles. In narcoleptic patients, the number of orexin neurons is greatly reduced, and orexin peptide levels in the cerebrospinal fluid are reduced to undetectable levels (Nishino et al., 2000; Peyron et al., 2000; Thannickal et al., 2000). Narcoleptic patients not only exhibit sleep fragmentation but also metabolic changes such as increases in body weight. Interestingly, mice lacking the orexin peptide develop narcolepsy-like symptoms (Chemelli et al., 1999),

Abbreviations: AAV, adeno-associated virus; Arc, arcuate nucleus; CNO, clozapine-N-oxide; DREADD, designer receptors exclusively activated by designer drugs; DTA, diphtheria toxin fragment A; ICV, intracerebroventricular; i.p., intraperitoneal; LHA, lateral hypothalamic area; NPY, neuropeptide Y; RER, respiratory exchange ratio; ZT, zeitgeber time.

* Corresponding author. Tel.: +81 52 789 3861; fax: +81 52 789 3889.
E-mail address: yamank@riem.nagoya-u.ac.jp (A. Yamanaka).

http://dx.doi.org/10.1016/j.neuropharm.2014.06.015

whereas orexin neuron-ablated transgenic mice develop hypophagia and late-onset obesity in addition to narcoleptic symptoms (Hara et al., 2001). Orexin neurons express not only orexins but also dynorphin (Chou et al., 2001) and glutamate (Abrahamson et al., 2001). Therefore, these differences in phenotype might suggest the involvement of other neurotransmitters besides orexin in the regulation of feeding and energy balance. Because it is unlikely that orexin peptides are the only factors released by orexin neurons *in vivo*, it is worth investigating the effects of selective manipulation of orexin neurons.

In this study, we generated a new *orexin-Cre* mouse line and employed a pharmacogenetic technique called designer receptors exclusively activated by designer drugs (DREADD) to selectively manipulate the activity of orexin neurons in free-moving mice. This method utilizes modified GPCRs to achieve selective, rapid and reversible modulation of neuronal activity. In short, muscarinic GPCRs are mutated so that their ability to bind their original ligand, acetylcholine, is lost while the synthetic ligand clozapine-N-oxide (CNO) can activate them (Armbruster et al., 2007). Gq-coupled DREADD, hM3Dq activates neurons through phospholipase C-dependent signal transduction (Alexander et al., 2009). Compared with optogenetic techniques utilizing ion channels, activation of GPCRs has a relatively longer effect on cellular signaling. Therefore, it is reasonable to employ DREADD to modulate the activity of orexin neurons for an extended time in order to examine the effects on feeding behavior and metabolism. We also selectively ablated orexin neurons using diphtheria toxin fragment A (DTA) to investigate the physiological roles of orexin neurons in feeding behaviors and metabolism.

Our results show that selective activation of orexin neurons simultaneously affects feeding behaviors and metabolism and that only 30% of orexin neurons are required to maintain such functions. These findings demonstrate the robust and concurrent regulation of feeding behaviors and wakefulness by orexin neurons.

2. Materials and methods

2.1. Animal usage

All experimental procedures involving animals were approved by the Institutional Animal Care and Use Committee of Research Institute of Environmental Medicine, Nagoya University. Mice were maintained under a strict 12 h light: dark cycle (light period: 8:00–20:00; dark period: 20:00–8:00) in a temperature-controlled room (22 °C). Food and water were available *ad libitum* except for in the experiments shown in Fig. 4. All efforts were made to minimize animal suffering and discomfort and to reduce the number of animals used.

2.2. Generation of orexin-Cre mice

The transgene was constructed with a 3.2-kb fragment of the 5′-upstream region of the human prepro-orexin gene as a promoter, Cre recombinase cDNA fused to EGFP with the 2A peptide, and the murine protamine-1 gene intron and poly(A) fragment (Fig. 1A). The transgene was excised and microinjected into pronuclei of fertilized mouse eggs (C57BL/6J mice) to generate transgenic founders. Founders were bred with C57BL/6J mice to produce stable *orexin-Cre* transgenic lines. Five transgene-positive founders were obtained from the *orexin-Cre* transgenic mice. Analysis of the N1 generation demonstrated that only two lines showed sufficient expression of Cre recombinase. The *orexin-Cre* transgenic mouse line that showed the highest Cre expression in orexin neurons was used for subsequent experiments.

2.3. Adeno-associated virus (AAV) production and purification

All AAV vectors were produced using the AAV Helper-Free System (Agilent Technologies, Inc., Santa Clara, CA, USA), and purified according to published methods (Lazarus et al., 2011). Briefly, HEK293 cells were transfected with a pAAV vector plasmid that included a gene of interest, pHelper, and pAAV-RC (serotype 10; provided by Penn Vector Core) using a standard calcium phosphate method. Three days later, the transfected cells were collected and suspended in artificial CSF (124 mM NaCl, 3 mM KCl, 26 mM $NaHCO_3$, 2 mM $CaCl_2$, 1 mM $MgSO_4$, 1.25 mM KH_2PO_4, 10 mM D-Glucose). After 4 freeze–thaw cycles, the cell lysate was treated with benzonase nuclease (Merck, Darmstadt, Germany) at 45 °C for 15 min, and centrifuged 2 times at 16,000 *g* for 10 min. The supernatant was used as the virus-containing solution. To measure the titer of purified virus dissolved in artificial CSF, quantitative PCR was performed; the virus was stored at −80 °C in aliquots before use. The pAAV-hSyn-FLEX-hM3Dq-mCherry plasmid was purchased from Addgene (ID: 44361).

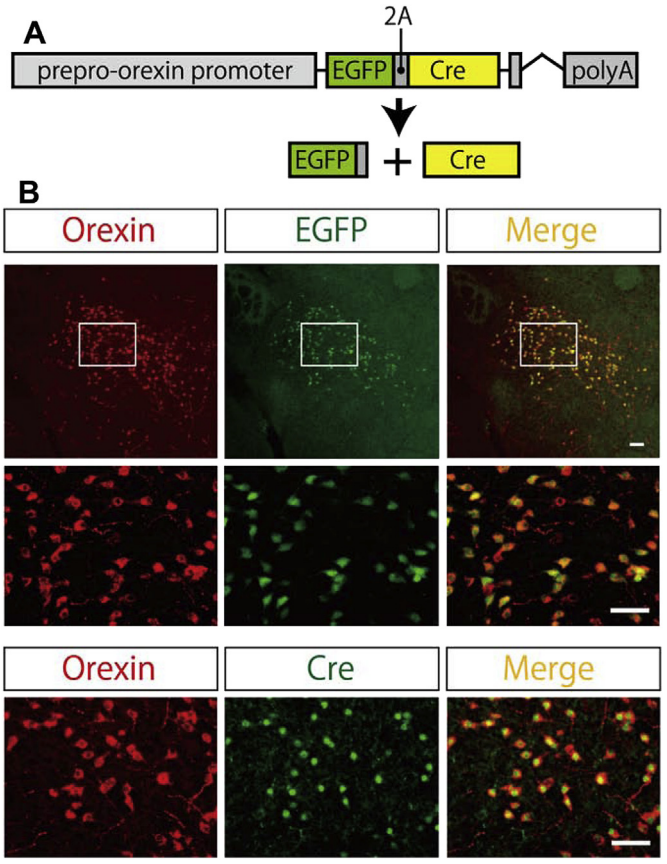

Fig. 1. Generation of *orexin-Cre* mice that express EGFP and Cre recombinase exclusively in orexin neurons. A: Schematic representation of the *orexin-Cre* transgene. To achieve orexin neuron-specific expression of Cre recombinase, we used a 3.2 kb 5′-upstream region of human prepro-orexin gene as a promoter. The transgene consists of the orexin promoter, EGFP-2A-Cre cDNA, and mouse protamine intron and poly(A) signal. Viral 2A peptide is cleaved just after translation, and EGFP and Cre recombinase localize independently. B: Specific expression of EGFP and Cre recombinase in orexin neurons. Immunohistochemistry showed specific expression of EGFP or Cre recombinase in orexin neurons in the LHA. Quantitative analysis showed 91.2 ± 0.9% ($n = 8$) colocalization of Cre recombinase with orexin. Scale bars, 100 μm (upper row) and 50 μm (middle and lower row).

2.4. Stereotaxic AAV injection

Surgeries for AAV injections were conducted under pentobarbital anesthesia (50 mg/kg, i.p.) using a stereotaxic instrument (David Kopf Instruments, Tujunga, CA, USA). Eight-week-old mice were injected stereotaxically into the LHA with recombinant AAV-hSyn-FLEX-hM3Dq-mCherry (600 nl/injection, 3×10^{12} copies/ml) or AAV-hSyn-FLEX-diphtheria toxin A fragment (DTA) (600 nl/injection, 3×10^{12} copies/ml) with a glass micropipette and an air pressure injector system (Pneumatic PicoPump; World Precision Instruments, Inc., Sarasota, FL, USA). Injection sites were as follows: bregma 1.5 mm, lateral ±0.7 mm, ventral −5.0 mm, for AAV-hSyn-FLEX-hM3Dq-mCherry; and bregma 1.5 mm, lateral ±0.5 mm, ventral 5.2 mm and 4.9 mm; bregma 1.5 mm, lateral ±0.9 mm, ventral −5.0 mm, for AAV-CMV-FLEX-DTA. Four weeks after the AAV injection, mice were analyzed using the Comprehensive Laboratory Animal Monitoring System (CLAMS; Columbus Instruments, Columbus, OH, USA).

2.5. Analysis of feeding behaviors and metabolism

Locomotion, food intake, water intake, and the RER were concurrently recorded using CLAMS. CLAMS is a set of live-in cages for automated, non-invasive, and simultaneous monitoring of horizontal and vertical activity, feeding and drinking, oxygen consumption, and CO_2 production. Twelve-week-old mice were individually placed in CLAMS cages and monitored for more than 5 days. The first 3 days were used as an acclimation period. Food and water consumption were measured directly

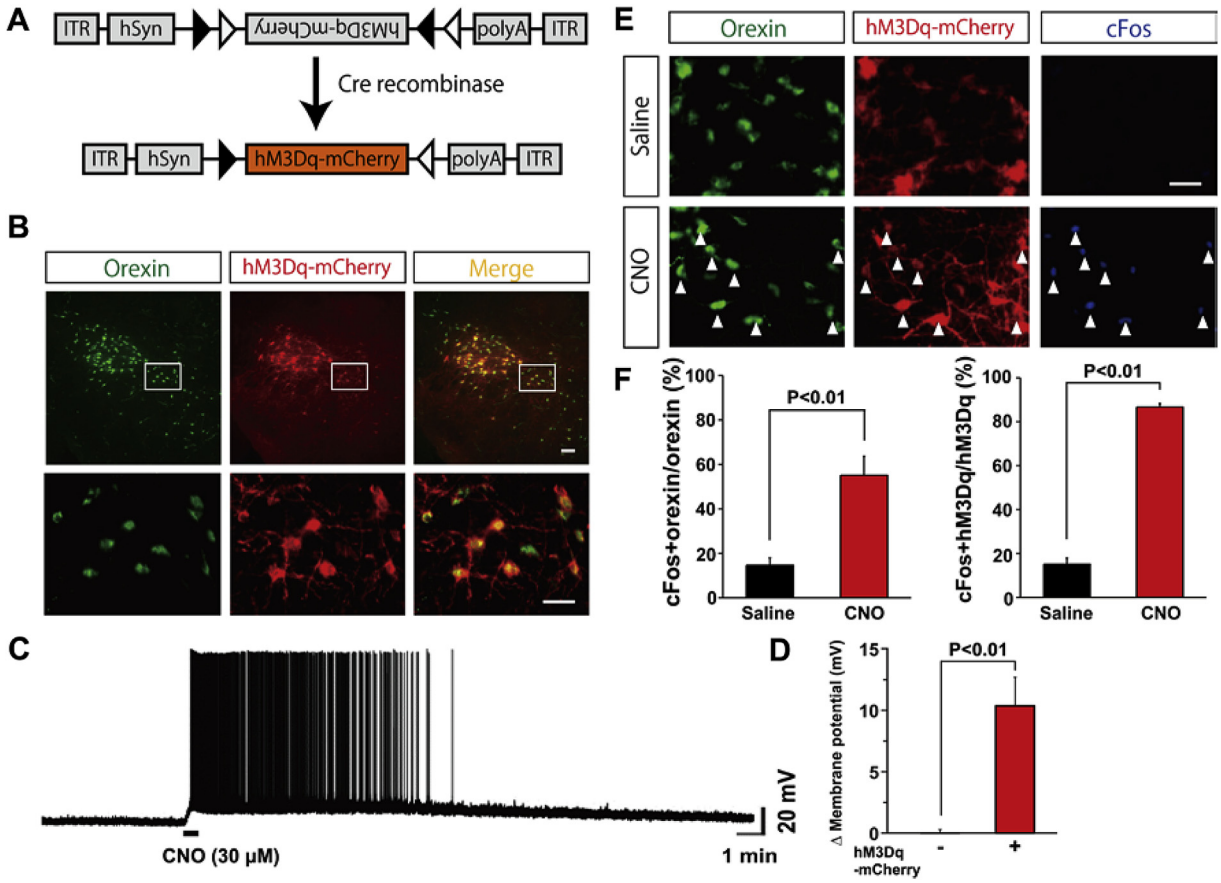

Fig. 2. Pharmacogenetic activation of orexin neurons by hM3Dq. A: Schematic representation of the AAV vector expressing hM3Dq with a FLEX switch. ITR, inverted terminal repeat; hSyn, human synapsin promoter. B: Coronal brain sections at the level of LHA, prepared from *orexin-Cre* mice 4 weeks after injection of AAV-hSyn-FLEX-hM3Dq-mCherry. Immunohistochemistry showed co-localization of hM3Dq with orexin. Scale bars, 100 μm (upper row) and 50 μm (lower row). C: Whole-cell, current clamp recording from an orexin neuron identified by mCherry fluorescence from an *orexin-Cre* mouse injected with AAV-hSyn0FLEX-hM3Dq-mCherry. CNO (30 μM) induced rapid depolarization of membrane potential and greatly increased the firing rate. D: ΔMembrane potential of the neurons administered CNO. CNO did not affect the membrane potential of neurons that did not express hM3Dq-mCherry. E: Injection of CNO *in vivo* induces c-Fos immunoreactivity in orexin neurons. Mice were sacrificed for c-Fos analysis 90 min after injection of saline or CNO (1.0 mg/kg, i.p.). Scale bar, 50 μm. F: Quantitative analysis of c-Fos activation of neurons at ZT13.5 in *orexin-Cre* mice injected with the hM3Dq AAV vector and administered saline or CNO at ZT 12 ($n = 7$).

by accumulated data, and XY ambulatory activity (a minimum of 3 different, consecutive horizontal beam breaks in counts) was used as the locomotion index. Data were taken every 10 min. Only male mice were used in the experiments. Blood glucose was measured using the ACCU-CHEK Nano meter (Roche Ltd., Basel, Switzerland). Blood samples (5 μl) were obtained by carefully pricking the tail vein using a sterile needle.

2.6. Immunohistochemistry

The mice were deeply anesthetized with isoflurane and transcardially perfused with 20 ml of chilled saline, followed by 20 ml of chilled 10% formalin solution (Wako Pure Chemical Industries, Ltd., Osaka, Japan). The brain was removed, post-fixed in 10% formalin solution at 4 °C overnight, and immersed in 30% sucrose in PBS at 4 °C for at least 2 days. A series of 40 μm sections were obtained with a cryostat (Leica CM3050 S; Leica Microsystems, Wetzlar, Germany).

For staining, coronal brain sections were immersed in blocking buffer (1% BSA and 0.25% Triton-X in PBS), then incubated with primary antibodies at 4 °C overnight. The sections were washed with blocking buffer then incubated with secondary antibodies for 1 h at RT. The brain sections were mounted and examined with a fluorescence microscope (BZ-9000, Keyence, Osaka, Japan or IX71, Olympus, Tokyo, Japan). Primary antibodies and secondary antibodies were diluted in blocking buffer as follows: anti-Cre recombinase rabbit antibody (Clontech Laboratories, Inc., Mountain View, CA, USA) at 1:500, anti-c-Fos rabbit antibody (Santa Cruz Biotechnology, Inc., Dallas, TX, USA) at 1:500, anti-orexin-A goat antibody (Santa Cruz) at 1:2000, anti-MCH rabbit antibody (Sigma–Aldrich, St. Louis, MO, USA) at 1:2000, CF 488-conjugated anti-mouse or anti-rabbit antibody (Biotium Inc., Hayward, CA, USA) at 1:1000, CF 594-conjugated anti-rabbit or anti-goat antibody (Biotium) at 1:1000 and CF 647-conjugated anti-goat antibody (Biotium) at 1:1000.

2.7. Electrophysiology

Three-week-old *orexin-Cre* mice were injected with AAV-hSyn-FLEX-hM3Dq-mCherry and sacrificed at 10 weeks of age. The mice were deeply anesthetized with isoflurane (Abbott Japan, Tokyo, Japan) and decapitated. Brains were quickly isolated in ice-cold cutting solution consisting of (in mM): 280 sucrose, 2 KCl, 10 HEPES, 0.5 $CaCl_2$, 10 $MgCl_2$, 10 glucose, pH 7.4 with NaOH, bubbled with 100% O_2, and immediately cut coronally into 350 μm-thick slices with a microtome (VTA-1200S, Leica Microsystems, Wetzlar, Germany). Slices containing the LHA were transferred to an incubation chamber filled with physiological solution containing (in mM): 135 NaCl, 5 KCl, 1 $CaCl_2$, 1 $MgCl_2$, 10 HEPES, 10 glucose, pH 7.4 with NaOH, bubbled with 100% O_2. The brain slices were then transferred to a recording chamber (RC-27L, Warner Instruments, Hamden, CT, USA) on a fluorescence microscope stage (BX51WI; Olympus, Tokyo, Japan). The fluorescence microscope was equipped with an infrared camera (C2741-79; Hamamatsu Photonics, Hamamatsu, Japan) for infrared differential interference contrast imaging and a CCD camera (IK-TU51CU, Olympus, Tokyo, Japan). Neurons with mCherry fluorescence were categorized as orexin neurons and were subjected to electrophysiological recordings. Recordings were performed with an Axopatch 200B amplifier (Molecular Devices LLC, Sunnyvale, CA, USA) using a borosilicate pipette (GC150-10; Harvard Apparatus, Holliston, MA, USA) prepared by a micropipette puller (P-1000; Sutter Instruments, Novato, CA, USA) filled with intracellular solution (4–10 MΩ), consisting of the following (in mM): 138 K-gluconate, 8 NaCl, 10 HEPES, 0.2 EGTA-Na_3, 2 MgATP, and 0.5 Na_2GTP, pH 7.3 with KOH. During recordings, cells were superfused with extracellular solution at a rate of 1.6 ml/min using a peristaltic pump (Dynamax; Rainin Instrument LLC, Oakland, CA, USA). CNO (Sigma–Aldrich) was dissolved in extracellular solution at a concentration of 30 μM and applied by local application through a fine tube (100 μm diameter) positioned near the recording neurons. The output signal was low-pass filtered at 5 kHz and digitized at 10 kHz. Data were recorded on a computer through a Digidata 1322A A/D converter using pClamp software (version 10;

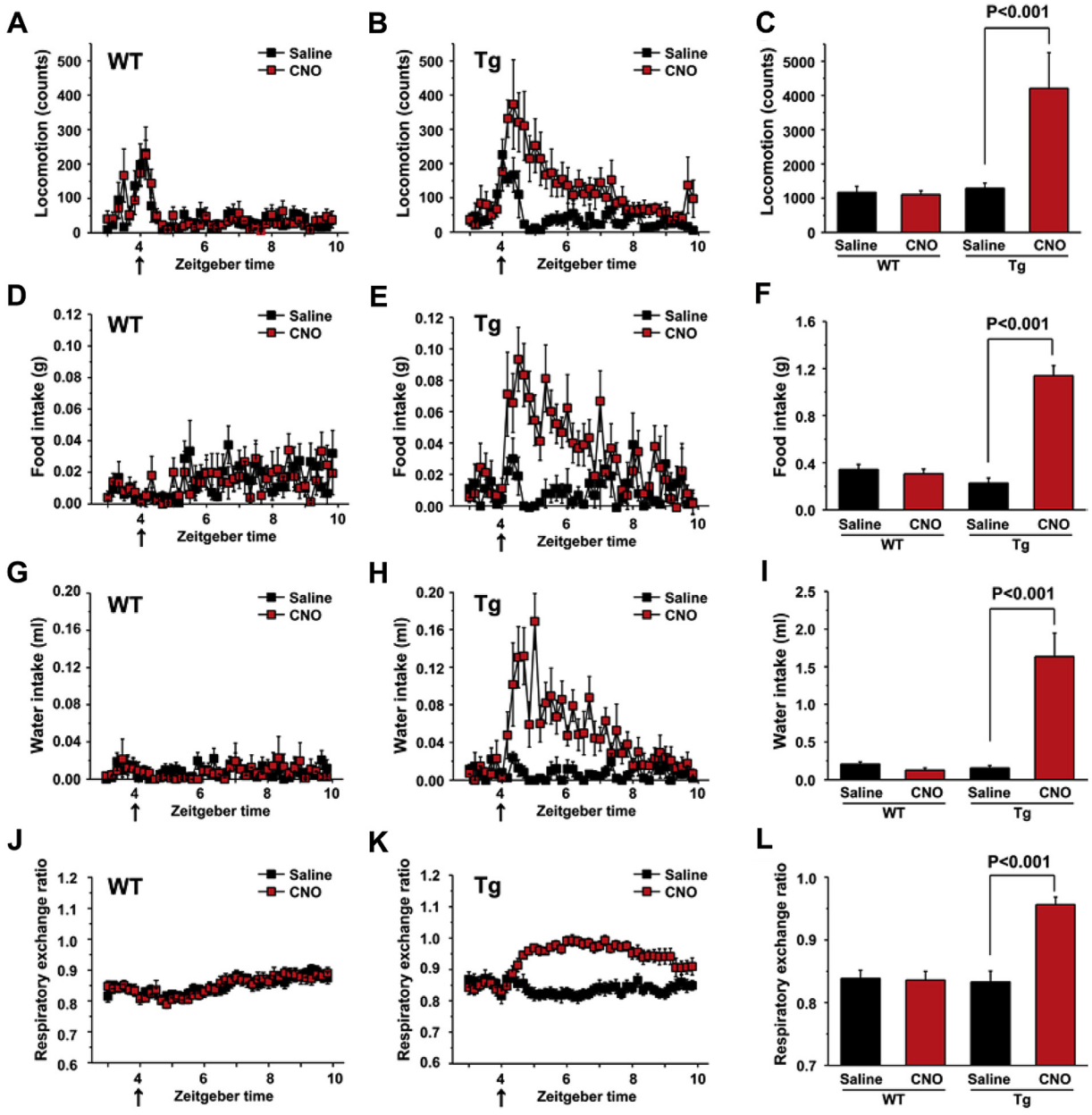

Fig. 3. Transient activation of orexin neurons alters locomotion, food intake, water intake and RER. *Orexin-Cre* or wild type mice were injected with AAV-hSyn-FLEX-hM3Dq-mCherry in the LHA. After 4 weeks, to allow for gene expression, they were injected with CNO (1.0 mg/kg, i.p.) or saline at 12:00 (ZT4). All mice were monitored using a comprehensive laboratory animal monitoring system (CLAMS), which continuously records activity. A–C: Ambulatory locomotion activity, D–F: Food intake, G–I: Water intake, and J–L: Respiratory exchange ratio. Data measured during 10 min intervals are plotted as mean ± SEM (WT, $n = 15$; Tg, $n = 9$) in the left and middle columns. The summation (C, F and I) or average (L) of each plot during the 4 h (from ZT 4 to ZT 8) is analyzed in the right column. The data were analyzed by one-way ANOVA followed by Tukey–Kramer multiple comparison tests.

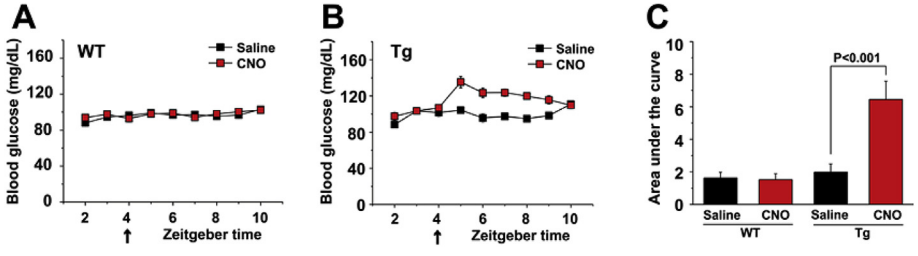

Fig. 4. Transient activation of orexin neurons alters blood glucose in fasting mice. *Orexin-Cre* or wild type mice were injected with AAV-hSyn-FLEX-hM3Dq-mCherry in the LHA at 8 weeks old. After 4 weeks they were injected with CNO (1.0 mg/kg, i.p.) or saline at 12:00 (ZT4). Measurements at 12:00 were done just before CNO/saline injection. All the mice were fasted from 20:00 (ZT12) on the day before the experiments. A, B: The time course of fasting blood glucose before and after i.p. injection of saline or CNO into *orexin-Cre* and wild type mice infected with AAV vectors. Measured data are plotted as mean ± SEM (WT, $n = 15$; Tg, $n = 9$). C: Quantitative analysis of average blood glucose during 4 h from ZT5 to ZT8. The data were analyzed by one-way ANOVA followed by Tukey–Kramer tests.

Molecular Devices). Traces were processed for presentation using Origin 9 software (LightStone, Tokyo, Japan) and Canvas14 software (ACD Systems, Victoria, Canada).

2.8. Statistics

Statistical analyses were performed using ORIGIN 9 software (LightStone). Simple comparisons of the means and SEM were performed by Student's *t*-test. Multiple comparisons of the means and SEM were performed by one-way ANOVA analyses followed by Tukey–Kramer post-hoc tests. A *P* value of less than 0.05 was considered significant in these studies.

3. Results

3.1. Cre recombinase is exclusively expressed in orexin neurons in novel orexin-Cre mice

To achieve specific expression in orexin neurons, we first generated a novel *orexin-Cre* mouse line. The utility of the 3.2 kb fragment of the 5′-upstream region of the human prepro-orexin gene for expressing genes of interest in orexin neurons has been previously reported (Sakurai et al., 1999; Moriguchi et al., 2002; Tsunematsu et al., 2011), so we employed this sequence as a promoter (Fig.1A). The Cre recombinase was fused to EGFP with a self-cleaving 2A peptide from the *Thosea asigna* virus to easily recognize orexin neurons by fluorescence without immunostaining. The viral 2A peptide is immediately cleaved upon translation, which allows expression of multiple proteins from a single ORF (Szymczak et al., 2004). The transgene was excised and microinjected into pronuclei of fertilized C57BL/6J mouse eggs to generate transgenic founders. Founders were bred with C57BL/6J mice to produce stable *orexin-Cre* transgenic lines. Five transgene-positive founders were obtained from the *orexin-Cre* transgenic mice. Analysis of the N1 generation demonstrated that only two lines showed sufficient expression of Cre recombinase. The *orexin-Cre* transgenic line that showed the highest Cre expression in orexin neurons was used in subsequent experiments.

Histological sections were examined from regions throughout the brain of *orexin-Cre* mice, and EGFP-expressing cells were found exclusively in the LHA. Immunohistochemistry with anti-Cre recombinase and anti-orexin-A antibody showed 91.2 ± 0.9% ($n = 8$) co-localization of Cre recombinase with orexin (Fig. 1B). No ectopic expression of EGFP or Cre recombinase was observed. Note that Cre recombinase was localized to the nucleus because of its nuclear localization signal at the N-terminus, while EGFP was localized throughout the soma. This finding demonstrates their successful separation by 2A peptide cleavage.

3.2. Expression and pharmacogenetic activation of hM3Dq in orexin neurons

To selectively manipulate activity of orexin neurons, we employed designer receptors exclusively activated by designer drugs (DREADD) technology. We used a Cre-dependent adeno-associated viral vector to specifically target the stimulatory hM3Dq DREADD to orexin neurons. The hM3Dq receptor has a high affinity for the synthetic ligand CNO (Alexander et al., 2009), and CNO administration can induce depolarization and firing of hM3Dq-expressing neurons. Stable transgene inversion was achieved by employing a FLEX (flip-excision) switch. The FLEX switch consists of paired loxP and lox2272 sequences and enables the expression of a gene of interest only when Cre recombinase is present (Atasoy et al., 2008) (Fig. 2A). Fused mCherry was used to monitor the expression of hM3Dq.

AAV-hSyn-FLEX-hM3Dq-mCherry was stereotaxically injected into the LHA of eight-week-old *orexin-Cre* mice, and mice were sacrificed 4 weeks after injection. Immunohistochemistry showed that hM3Dq was expressed exclusively in orexin neurons (Fig. 2B). Using fused mCherry as a marker, 71.3 ± 6.8% ($n = 7$) of orexin neurons were shown to express hM3Dq-mCherry.

We then performed whole-cell current clamp recordings to determine the ability of hM3Dq to activate orexin neurons *in vitro*. *Orexin-Cre* mice were injected with AAV-hSyn-FLEX-hM3Dq-mCherry in the LHA at 3 weeks of age, and were sacrificed 7 weeks after injection to obtain brain slices. Neurons strongly expressing mCherry were considered to be orexin neurons and were subjected to whole-cell recordings. Local application of CNO (30 μM) to brain slices greatly increased the firing rate of orexin neurons (Fig. 2C). This CNO-induced depolarization was sustained for about 10 min after washout, and was reversible. We also confirmed that application of CNO did not affect the membrane potential of orexin neurons not expressing hM3Dq-mCherry ($P < 0.01$; Student's *t*-test; $n = 5$) (Fig. 2D).

Next, we checked the neuronal activation by hM3Dq *in vivo*. Neuronal activity of orexin neurons changes in accordance with arousal state; c-Fos expression in orexin neurons is low during the light period and high during the dark period (Estabrooke et al., 2001). Therefore, we examined the effects of excitatory hM3Dq DREADD during the light period when daily activity of orexin neurons is at its lowest. *Orexin-Cre* mice were injected with AAV-hSyn-FLEX-hM3Dq-mCherry into the LHA at 8 weeks of age. Wild type mice were also injected with the same AAV vectors as a control. 4 weeks after stereotaxic injection, mice were administered CNO (1.0 mg/kg) by i.p. injection at 12:00 (ZT4), and sacrificed at 13:30 (ZT5.5). We found that i.p. injection of CNO greatly increased c-Fos immunoreactivity in orexin neurons expressing hM3Dq-mCherry (Fig. 2E). Quantitative analyses showed that 55.1 ± 8.5% of orexin-ir neurons expressed c-Fos in *orexin-Cre* mice injected with CNO ($n = 7$). This expression level of c-Fos was much higher than that in the mice administered saline (14.7 ± 3.3%) ($P < 0.01$; Student's *t*-test; $n = 7$) (Fig. 2F). Note that the c-Fos expression rate was increased to 86.7 ± 7.2% if orexin-ir neurons expressing hM3Dq-mCherry were analyzed ($n = 7$) (Fig. 2F). In wild type mice infected with AAV-hSyn-FLEX-hM3Dq-mCherry, no expression of mCherry was detected. We also confirmed that c-Fos immunoreactivity showed no difference between the wild type mice injected with CNO and saline (data not shown).

3.3. Activation of orexin neurons alters feeding behaviors and metabolism

After the confirmation of selective activation of orexin neurons, we examined the effects of pharmacogenetic activation of orexin neurons on feeding behaviors and metabolism. We employed a CLAMS to simultaneously monitor locomotion, food intake, water intake, and respiratory exchange ratio. The effects of hM3Dq were examined at 12:00 (ZT4) when the activity of orexin neurons is lowest. Saline injection into *orexin-Cre* mice expressing hM3Dq-mCherry (Tg) was used as the control, and CNO injection into wild-type mice infected with AAV-hSyn-FLEX-hM3Dq-mCherry (WT) was used as an additional control.

Although i.p. injection of saline activated locomotor activity in control mice during the first 30 min after injection (Fig. 3A), stimulation of orexin neurons by i.p. injection of CNO (1.0 mg/kg) induced a significantly greater increase in locomotion compared with controls (Fig. 3B). This increase in locomotion started immediately after injection, and was sustained for about 4 h. One-way ANOVA and Tukey–Kramer post-hoc tests showed that CNO administration into Tg mice significantly increased locomotor activity during the 4 h after injection ($P < 0.001$; WT, $n = 15$; Tg, $n = 9$) (Fig. 3C). The total number of locomotive counts among Tg mice injected with CNO was 4-fold more than in controls (Tg + CNO; 4206 ± 1045 counts, Tg + Saline; 1295 ± 148 counts).

Pharmacogenetic activation also affected food intake. While i.p. injection of saline into WT and Tg mice induced only weak effects on feeding (Fig. 3D), CNO administration into Tg mice rapidly increased food intake (Fig. 3E). This rapid increase in food intake was first recorded within 10 min after injection, and was sustained for approximately 4 h (Fig. 3E). One-way ANOVA and Tukey–Kramer post-hoc tests showed that CNO administration into Tg mice resulted in a significant increase in food intake during the 4 h after injection ($P < 0.001$; WT, $n = 15$; Tg, $n = 9$) (Fig. 3F). The average food intake in orexin neuron-activated mice was 5-fold greater than in saline controls (Tg + CNO; 1.14 ± 0.08 g, Tg + Saline; 0.23 ± 0.04 g).

The effect of pharmacogenetic activation of orexin neurons on water intake was more prominent. Saline injection resulted in almost no change (Fig. 3G), while i.p. injection of CNO into Tg mice induced a strong increase in water intake (Fig. 3H). The increase in water intake also started within the first 10 min after injection, and was sustained for about 4 h, similar to the changes in locomotion and food intake. One-way ANOVA and Tukey–Kramer post-hoc tests showed that CNO administration into Tg mice significantly increased water intake during the 4 h after injection ($P < 0.001$; WT, $n = 15$; Tg, $n = 9$) (Fig. 3I), and the average water intake in orexin neuron-activated mice was 10-fold greater than in saline controls (Tg + CNO; 1.64 ± 0.31 ml, Tg + Saline; 0.16 ± 0.03 ml).

We also found that CNO injection alters metabolic parameters in Tg mice. Injection of saline into Tg mice or CNO injection into WT mice had little effect on the respiratory exchange ratio (RER) (Fig. 3J). In contrast, RER strongly increased after injection of CNO in Tg mice. This change was not as pronounced as the change in locomotion or feeding, but continued even after the change in locomotion had returned to basal levels (Fig.3K). One-way ANOVA and Tukey–Kramer post-hoc tests showed that CNO administration into hM3Dq-expressing mice significantly increased average RER during the 4 h after injection ($P < 0.001$; WT, $n = 15$; Tg, $n = 9$) (Fig. 3L).

To examine metabolic changes, we also investigated blood glucose levels in transgenic mice. Because pharmacogenetic activation of orexin neurons increases food intake, we removed access to food at 20:00 on the day before the investigation to exclude indirect effects of food digestion on blood glucose levels. We found that i.p. injection of CNO (1.0 mg/kg) increased blood glucose independently from food intake (Fig. 4B) and this effect was maintained for about 6 h. In contrast, injection of saline into Tg mice or CNO into WT mice had little effect on blood glucose levels (Fig. 4A). ANOVA and Tukey's post-hoc tests showed that CNO administration into hM3Dq-expressing mice resulted in a significant increase in the AUC (area under the curve) during the 6 h after injection ($P < 0.001$; WT, $n = 15$; Tg, $n = 9$) (Fig. 4C).

3.4. Selective ablation of orexin neurons by DTA

To investigate the physiological role of orexin neurons in feeding and metabolism, we employed selective ablation of orexin neurons using DTA. We produced Cre-dependent AAV vectors that selectively induce DTA expression only in cells expressing Cre recombinase (AAV-CMV-FLEX-DTA) (Fig. 5A). DTA catalyzes ADP-ribosylation of eukaryotic elongation factor 2 (Oppenheimer and Bodley, 1981), and causes cell death by inhibiting protein synthesis. We stereotaxically injected AAV-CMV-FLEX-DTA vectors into the LHA of eight-week-old *orexin-Cre* mice, and sacrificed them 4 weeks after injection. Immunohistochemistry with anti-orexin-A antibody showed strong ablation of orexin neurons (Fig. 5B). To confirm whether this ablation of orexin neurons was selective, we also performed immunostaining of melanin-concentrating hormone (MCH) neurons as a control. MCH neurons are also localized in the LHA similar to orexin neurons, although their localization is completely segregated. We found that MCH neurons were mostly intact, while orexin neurons were strongly ablated at the same position (Fig. 5B).

We divided orexin neuron-ablated mice into 2 groups since we used 2 different lots of AAV-CMV-FLEX-DTA and there were differences in the resulting extent of ablation. One group was labeled "DTA (70%)" mice as 69.6 ± 2.4% of orexin neurons were ablated in this group, $n = 8$; the other group was labeled "DTA (83%)" mice as 83.0 ± 1.7% of orexin neurons were ablated in this group, $n = 8$.

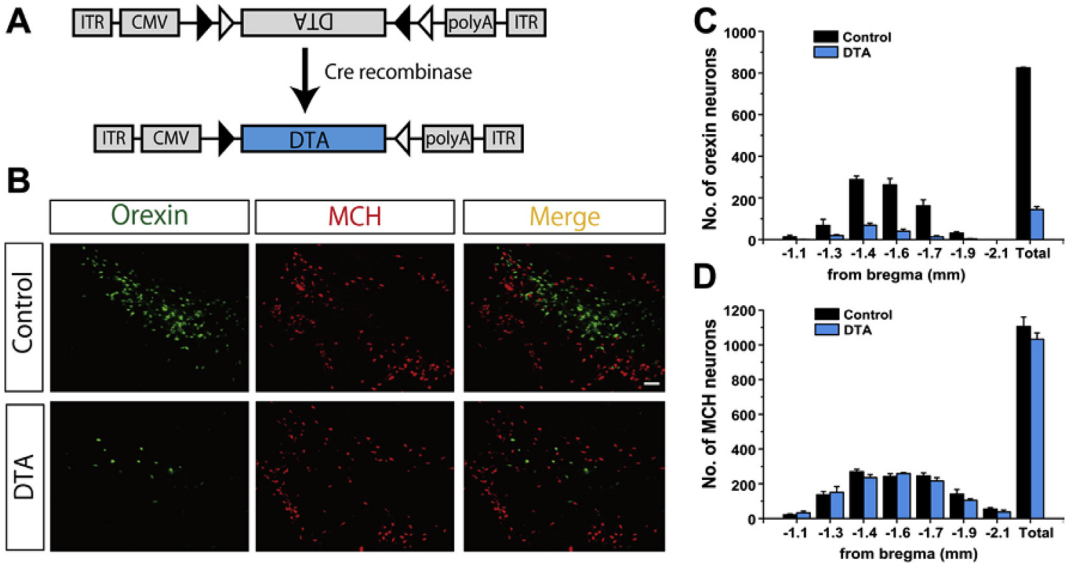

Fig. 5. Selective ablation of orexin neurons by DTA. A: Schematic representation of double-floxed Cre-dependent AAV vector expressing DTA. ITR, inverted terminal repeat; hSyn, human synapsin promoter. B: Coronal brain sections at the level of LHA, prepared from *orexin-Cre* mice 4 weeks after injection of AAV-CMV-FLEX-DTA. Immunohistochemistry showed that orexin neurons were strongly ablated, while MCH neurons were intact at the same position. C: Quantitative analysis of the number of orexin and D: MCH neurons 4 weeks after the injection of AAV-CMV-FLEX-DTA into *orexin-Cre* mice. 83.0 ± 1.7% ($n = 8$) of orexin neurons were ablated, while the number of MCH neurons did not change compared with control mice. The data were analyzed by Student's *t*-test.

Quantitative analyses confirmed that the number of MCH neurons in DTA (83%) mice did not change significantly compared with control mice (93.4 ± 3.2%, $n = 8$) (Fig. 5C and D).

3.5. Feeding behaviors and metabolism in orexin neuron-ablated mice

After the confirmation of selective ablation of orexin neurons, we examined feeding behaviors and metabolism in these orexin neuron-ablated mice using CLAMS. Eight-week-old *orexin-Cre* mice injected with AAV-CMV-FLEX-DTA (DTA (70%) mice and DTA (83%) mice) or AAV-CMV-FLEX-mCherry vectors (control mice) were analyzed by CLAMS at 12 weeks of age. At least 3 days were allowed for acclimation before sampling the data.

We found that the time course of locomotion in DTA (83%) mice was similar to that in control mice. No strong reciprocal changes between the dark and light periods were observed. Quantitative analysis of total locomotive activity showed a weak decreasing trend in both the light period and dark period, although these differences were not statistically significant (Fig. 6A).

DTA (83%) mice showed a significant decrease in food intake during the light period (one-way ANOVA and Tukey–Kramer post-hoc tests; $P < 0.05$; $n = 8$) (Fig. 6B). The total amount of food intake by DTA (83%) mice during the dark period was also lower compared to controls, although the difference was not significant. Note that changes in food intake in DTA (83%) mice during the transition from the light to dark period were slightly reduced compared with control mice.

Most strikingly, water intake was strongly reduced in DTA (83%) mice throughout the entire day (one-way ANOVA and Tukey–Kramer post-hoc tests; $P < 0.05$; $n = 8$) (Fig. 6C). This overall decrease in water intake was largely attributed to a decrease during the dark period (one-way ANOVA and Tukey–Kramer post-hoc tests; $P < 0.01$; $n = 8$), although water intake during the light period was also less than in control mice. Locomotion, food intake, and water intake in DTA (70%) mice were not significantly changed compared with control mice (Fig. 6A, B and C). Note that these reductions in food and water intake were present even though the average body weight of DTA (83%) mice was significantly larger than control mice ($P < 0.01$; $n = 8$; one-way ANOVA followed by Tukey–Kramer tests) (Fig. 7A). Body weight was measured at 12 weeks of age, 4 weeks after injection of AAV vectors. In addition, blood glucose levels of DTA (83%) and DTA (70%) mice were lower than control mice (Fig. 7B).

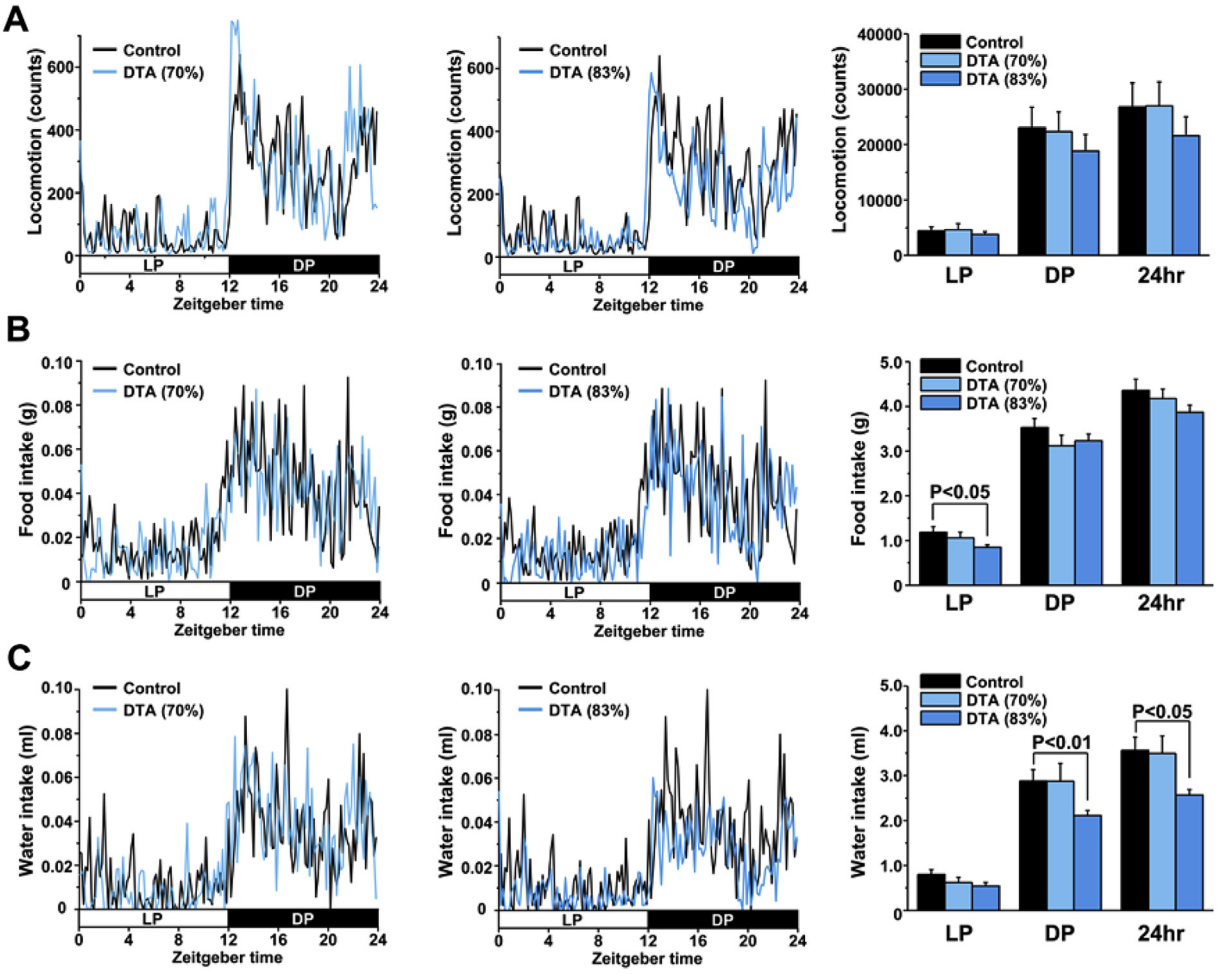

Fig. 6. Ablation of orexin neurons by DTA diminished food intake and water intake. *Orexin-Cre* mice were injected with AAV-hSyn-FLEX-mCherry (Control) or AAV-CMV-FLEX-DTA (DTA) in the LHA. After 4 weeks, to allow for gene expression, they were analyzed using a comprehensive laboratory animal monitoring system (CLAMS), which continuously records activity. A: Ambulatory locomotion activity, B: Food intake, and C: Water intake. Measured data are plotted as mean ± SEM ($n = 8$). The summations of each plot during LP (from ZT 0 to 12), DP (from ZT 12 to 24), and throughout an entire day were analyzed by one-way ANOVA followed by Tukey–Kramer tests. DTA (83%) mice showed decreased food and water intake.

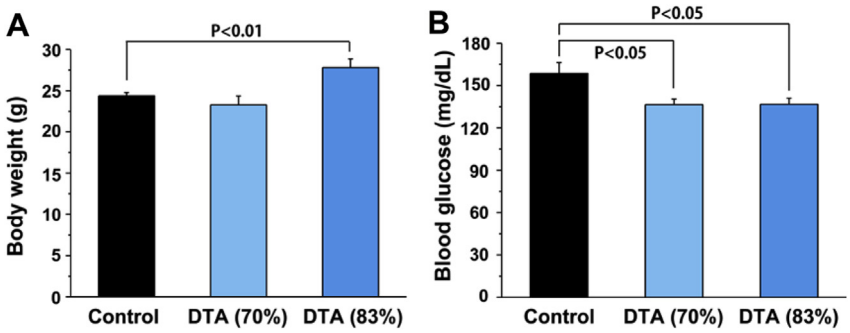

Fig. 7. Ablation of orexin neurons affects blood glucose and body weight. *Orexin-Cre* mice were injected with AAV-hSyn-FLEX-mCherry (Control) or AAV-CMV-FLEX-DTA (DTA) vectors in the LHA. After 4 weeks they were measured. A: Body weight and B: blood glucose. Measured data are plotted as mean ± SEM ($n = 8$). The data were analyzed by one-way ANOVA followed by Tukey–Kramer tests.

4. Discussion

The orexin system has been implicated in feeding behaviors and metabolism. ICV administration of orexin peptides induces feeding (Sakurai et al., 1998) and drinking behavior (Kunii et al., 1999) and also increases blood glucose via the sympathetic pathway (Yi et al., 2009). Our results using pharmacogenetics fundamentally confirm these roles in feeding and metabolism, but also indicate new insights that are described below. In addition, stable specific expression of Cre-dependent AAV vectors shows that our new *orexin-Cre* mice are a valuable tool for manipulating the orexin system *in vivo*.

4.1. The effects of manipulating orexin neuronal activity by DREADD

In this study we achieved selective activation of orexin neurons using pharmacogenetics. Stereotaxic injection of the AAV vector into the LHA of orexin-Cre mice induced sufficient expression of hM3Dq exclusively in orexin neurons, and neuronal activation by CNO was confirmed by electrophysiology and c-Fos immunohistochemistry. Activation of orexin neurons induced concurrent increases in locomotion, food intake, and water intake, and affected metabolic factors such as respiratory exchange ratio and blood glucose level. These findings enhance our understanding of the integrative function of orexin neurons on feeding and metabolism. As far as we know, this is the first study to comprehensively investigate the effects of manipulating orexin neuronal activity on feeding and metabolism.

The induction of elevated food and water intake was sustained for at least 4 h. It has been reported that activation of food and water intake by ICV administration of orexin peptides returned to baseline within 2 h (Kunii et al., 1999). Because the CNO (1.0 mg/kg; i.p.) used in this study is supposed to be cleared from blood plasma within 2 h (Guettier et al., 2009), it is possible that the longer-lasting effects of pharmacogenetic activation on feeding behaviors is derived from the activity of co-factors released along with orexins. However, other alternative explanations should be carefully considered. It was reported that activation of forebrain principal neurons by hM3Dq can induce very long effects on locomotion up to 9 h (Alexander et al., 2009). It was also reported that carbachol-induced gamma rhythm in hippocampal slices persists even after the removal of carbachol from the bath (Fisahn et al., 1998). Therefore, transient activation of muscarinic receptors (and hM3Dq) can induce persistent responses in some neurons.

The effect on blood glucose might be derived from activation of sympathetic nerves. Orexin can influence liver function via the sympathetic pathway (Van Den Top et al., 2003) and it has also been reported that the stimulatory effect on blood glucose by ICV administration of orexin-A was prevented by hepatic sympathetic denervation (Yi et al., 2009). Therefore, it is also possible that the sustained effects on blood glucose and RER by CNO result from the involvement of indirect signal transduction downstream of orexin neurons.

4.2. Sustained in vivo manipulation of metabolism by DREADD

Recently, a growing number of optogenetic studies have revealed the physiological functions of orexin neurons in the regulation of sleep and arousal (Adamantidis et al., 2007; Tsunematsu et al., 2011; Carter et al., 2012). However, it is difficult to alter sustained neuronal activity over a few hours using optogenetics due to inactivation of photo-activated channels or pumps. For example, our group found that optogenetic inhibition of orexin neurons by halorhodopsin was only sustained for a few minutes (Tsunematsu et al., 2011). Arch or ArchT are more stable than halorhodopsin, but they are still not able to inhibit neuronal activity for multiple hours. In addition, optogenetic activation depolarizes neurons in an extremely synchronized manner, which is not likely to happen under physiological conditions. Furthermore, channelrhodopsin2 is much more permeable to H^+ than Na^+, and its activation can induce intracellular acidification and affect cellular signaling (Beppu et al., 2014). Given these limitations of optogenetics, DREADD is a valuable alternative tool for manipulating endogenous signaling, although its time resolution is not as high.

In this study, pharmacogenetic activation of orexin neurons could alter RER and blood glucose for as long as 6 h. It was reported that cholecystokinin (CCK) activates orexin neurons through the cholecystokinin A receptor (Tsujino et al., 2005). CCK_A couples with the Gq subclass of G-proteins, and subsequently depolarizes membrane potential via activation of non-selective cation channels, likely TRP channels in orexin neurons. These pathways might be involved in hM3Dq-mediated activation of orexin neurons since hM3Dq is reported to activate the endogenous Gq pathway. The longer term effects and the facility of pharmacogenetics are suitable for various behavioral testing and physiological experiments (Ray et al., 2011; Krashes et al., 2013). Recently it was shown that manipulation of orexin neuronal activity by DREADD can affect states of sleep/wakefulness (Sasaki et al., 2011). Our study extends the application of DREADD to additional behaviors including feeding and metabolism. In addition, this pharmacogenetic technique does not require optic fibers for stimulation, so it is suitable for usage in closed cages for monitoring metabolic factors such as O_2 consumption or CO_2 emission.

4.3. Robust regulation of feeding behaviors by orexin neurons

Previous studies have shown that ablation of orexin neurons induces severe fragmentation of sleep/wakefulness cycles and late-onset obesity (Hara et al., 2001). Therefore, it is surprising that a 70% ablation of orexin neurons showed almost no change in these parameters. This finding implies that only a small percentage of orexin neurons are required to maintain their function in wakefulness, feeding behaviors, and metabolic regulation. It is known that more than 70% of dopaminergic neurons are lost in the substantia nigra pars compacta before the onset of Parkinson's disease (Lang and Lozano, 1998). In addition, postmortem studies of narcoleptic subjects indicated an 80–100% reduction in the number of orexin neurons, determined by *in situ* hybridization (Peyron et al., 2000). These findings suggest the robust regulation of feeding behavior and metabolism by orexin neurons.

Conversely, pharmacogenetic activation of orexin neurons showed strong effects, although the expression rate of hM3Dq was lower than that of DTA. It has been reported that orexin neurons express orexin receptors and can be activated by orexin peptides (Yamanaka et al., 2010). This positive feedback might explain the strong effects of pharmacogenetically activating orexin neurons observed in our study. It was reported that chronic administration of orexin-A does not affect body weight, although it increases daytime food intake (Yamanaka et al., 1999). Therefore, it is possible that chronic activation of the orexin system might not be sufficient to overcome the strong homeostasis of body weight *in vivo*.

It is also intriguing that an 83% loss of orexin neurons decreased feeding behaviors, while the pattern of locomotion in the mice remained intact. Various effects on feeding behaviors and physiological responses by orexin administration are sometimes regarded as the results of changes in wakefulness. However, the early emerging changes in food and water intake suggest that orexin neurons directly regulate feeding behaviors. In addition, we observed the first changes in locomotion and food or water intake simultaneously within 10 min after injection. These results also show that the changes in feeding by manipulation of orexin neuronal activities are not indirect effects induced by changes in sleep/wakefulness. Taken together, our findings indicate the robust and concurrent regulation of feeding behaviors and metabolism by orexin neurons.

Acknowledgments

This study was supported by a Grant-in-Aid for Scientific Research (B) (23300142) and a Grant-in-Aid for Scientific Research on Innovative Area "Mesoscopic Neurocircuitry" (23115103) (A.Y.), and by a Grant-in-Aid for Young Scientists (B) (26860157) and a Grant-in-Aid for Scientific Research on Innovative Area "The Evolutionary Origin and Neural Basis of the Empathetic Systems" (26118507) (A.I.), and by a Grant-in-Aid for Scientific Research (B) (24300129) and the World Premier International Research Center Initiative (WPI) from the Ministry of Education, Culture, Sports, Science, and Technology (M.L.). We thank C. Saito and K. Nishimura for technical assistance.

References

Abrahamson, E.E., Leak, R.K., Moore, R.Y., 2001. The suprachiasmatic nucleus projects to posterior hypothalamic arousal systems. Neuroreport 12, 435–440.
Adamantidis, A.R., Zhang, F., Aravanis, A.M., Deisseroth, K., De Lecea, L., 2007. Neural substrates of awakening probed with optogenetic control of hypocretin neurons. Nature 450, 420–424.
Alexander, G.M., Rogan, S.C., Abbas, A.I., Armbruster, B.N., Pei, Y., Allen, J.A., Nonneman, R.J., Hartmann, J., Moy, S.S., Nicolelis, M.A., Mcnamara, J.O., Roth, B.L., 2009. Remote control of neuronal activity in transgenic mice expressing evolved G protein-coupled receptors. Neuron 63, 27–39.
Armbruster, B.N., Li, X., Pausch, M.H., Herlitze, S., Roth, B.L., 2007. Evolving the lock to fit the key to create a family of G protein-coupled receptors potently activated by an inert ligand. Proc. Natl. Acad. Sci. U. S. A. 104, 5163–5168.
Atasoy, D., Aponte, Y., Su, H.H., Sternson, S.M., 2008. A FLEX switch targets Channelrhodopsin-2 to multiple cell types for imaging and long-range circuit mapping. J. Neurosci. 28, 7025–7030.
Beppu, K., Sasaki, T., Tanaka, K.F., Yamanaka, A., Fukazawa, Y., Shigemoto, R., Matsui, K., 2014. Optogenetic countering of glial acidosis suppresses glial glutamate release and ischemic brain damage. Neuron 81, 314–320.
Carter, M.E., Brill, J., Bonnavion, P., Huguenard, J.R., Huerta, R., De Lecea, L., 2012. Mechanism for Hypocretin-mediated sleep-to-wake transitions. Proc. Natl. Acad. Sci. U. S. A. 109, E2635–E2644.
Chemelli, R.M., Willie, J.T., Sinton, C.M., Elmquist, J.K., Scammell, T., Lee, C., Richardson, J.A., Williams, S.C., Xiong, Y., Kisanuki, Y., Fitch, T.E., Nakazato, M., Hammer, R.E., Saper, C.B., Yanagisawa, M., 1999. Narcolepsy in orexin knockout mice: molecular genetics of sleep regulation. Cell 98, 437–451.
Chou, T.C., Lee, C.E., Lu, J., Elmquist, J.K., Hara, J., Willie, J.T., Beuckmann, C.T., Chemelli, R.M., Sakurai, T., Yanagisawa, M., Saper, C.B., Scammell, T.E., 2001. Orexin (hypocretin) neurons contain dynorphin. J. Neurosci 21, RC168.
De Lecea, L., Huerta, R., 2014. Hypocretin (orexin) regulation of sleep-to-wake transitions. Front. Pharmacol. 5, 16.
De Lecea, L., Kilduff, T.S., Peyron, C., Gao, X., Foye, P.E., Danielson, P.E., Fukuhara, C., Battenberg, E.L., Gautvik, V.T., Bartlett 2nd, F.S., Frankel, W.N., Van Den Pol, A.N., Bloom, F.E., Gautvik, K.M., Sutcliffe, J.G., 1998. The hypocretins: hypothalamus-specific peptides with neuroexcitatory activity. Proc. Natl. Acad. Sci. U. S. A. 95, 322–327.
Estabrooke, I.V., Mccarthy, M.T., Ko, E., Chou, T.C., Chemelli, R.M., Yanagisawa, M., Saper, C.B., Scammell, T.E., 2001. Fos expression in orexin neurons varies with behavioral state. J. Neurosci. 21, 1656–1662.
Fisahn, A., Pike, F.G., Buhl, E.H., Paulsen, O., 1998. Cholinergic induction of network oscillations at 40 Hz in the hippocampus in vitro. Nature 394, 186–189.
Guettier, J.M., Gautam, D., Scarselli, M., Ruiz De Azua, I., Li, J.H., Rosemond, E., Ma, X., Gonzalez, F.J., Armbruster, B.N., Lu, H., Roth, B.L., Wess, J., 2009. A chemical-genetic approach to study G protein regulation of beta cell function in vivo. Proc. Natl. Acad. Sci. U. S. A. 106, 19197–19202.
Hara, J., Beuckmann, C.T., Nambu, T., Willie, J.T., Chemelli, R.M., Sinton, C.M., Sugiyama, F., Yagami, K., Goto, K., Yanagisawa, M., Sakurai, T., 2001. Genetic ablation of orexin neurons in mice results in narcolepsy, hypophagia, and obesity. Neuron 30, 345–354.
Inutsuka, A., Yamanaka, A., 2013. The physiological role of orexin/hypocretin neurons in the regulation of sleep/wakefulness and neuroendocrine functions. Front. Endocrinol. (Lausanne) 4, 18.
Krashes, M.J., Shah, B.P., Koda, S., Lowell, B.B., 2013. Rapid versus delayed stimulation of feeding by the endogenously released AgRP neuron mediators GABA, NPY, and AgRP. Cell Metab. 18, 588–595.
Kunii, K., Yamanaka, A., Nambu, T., Matsuzaki, I., Goto, K., Sakurai, T., 1999. Orexins/hypocretins regulate drinking behaviour. Brain Res. 842, 256–261.
Lang, A.E., Lozano, A.M., 1998. Parkinson's disease. First of two parts. N. Engl. J. Med. 339, 1044–1053.
Lazarus, M., Shen, H.Y., Cherasse, Y., Qu, W.M., Huang, Z.L., Bass, C.E., Winsky-Sommerer, R., Semba, K., Fredholm, B.B., Boison, D., Hayaishi, O., Urade, Y., Chen, J.F., 2011. Arousal effect of caffeine depends on adenosine A2A receptors in the shell of the nucleus accumbens. J. Neurosci. 31, 10067–10075.
Moriguchi, T., Sakurai, T., Takahashi, S., Goto, K., Yamamoto, M., 2002. The human prepro-orexin gene regulatory region that activates gene expression in the lateral region and represses it in the medial regions of the hypothalamus. J. Biol. Chem. 277, 16985–16992.
Nambu, T., Sakurai, T., Mizukami, K., Hosoya, Y., Yanagisawa, M., Goto, K., 1999. Distribution of orexin neurons in the adult rat brain. Brain Res. 827, 243–260.
Nishino, S., Ripley, B., Overeem, S., Lammers, G.J., Mignot, E., 2000. Hypocretin (orexin) deficiency in human narcolepsy. Lancet 355, 39–40.
Oppenheimer, N.J., Bodley, J.W., 1981. Diphtheria toxin. Site and configuration of ADP-ribosylation of diphthamide in elongation factor 2. J. Biol. Chem. 256, 8579–8581.
Peyron, C., Faraco, J., Rogers, W., Ripley, B., Overeem, S., Charnay, Y., Nevsimalova, S., Aldrich, M., Reynolds, D., Albin, R., Li, R., Hungs, M., Pedrazzoli, M., Padigaru, M., Kucherlapati, M., Fan, J., Maki, R., Lammers, G.J., Bouras, C., Kucherlapati, R., Nishino, S., Mignot, E., 2000. A mutation in a case of early onset narcolepsy and a generalized absence of hypocretin peptides in human narcoleptic brains. Nat. Med. 6, 991–997.
Peyron, C., Tighe, D.K., Van Den Pol, A.N., De Lecea, L., Heller, H.C., Sutcliffe, J.G., Kilduff, T.S., 1998. Neurons containing hypocretin (orexin) project to multiple neuronal systems. J. Neurosci. 18, 9996–10015.
Ray, R.S., Corcoran, A.E., Brust, R.D., Kim, J.C., Richerson, G.B., Nattie, E., Dymecki, S.M., 2011. Impaired respiratory and body temperature control upon acute serotonergic neuron inhibition. Science 333, 637–642.
Sakurai, T., 2007. The neural circuit of orexin (hypocretin): maintaining sleep and wakefulness. Nat. Rev. Neurosci. 8, 171–181.
Sakurai, T., Amemiya, A., Ishii, M., Matsuzaki, I., Chemelli, R.M., Tanaka, H., Williams, S.C., Richarson, J.A., Kozlowski, G.P., Wilson, S., Arch, J.R., Buckingham, R.E., Haynes, A.C., Carr, S.A., Annan, R.S., Mcnulty, D.E., Liu, W.S., Terrett, J.A., Elshourbagy, N.A., Bergsma, D.J., Yanagisawa, M., 1998. Orexins and orexin receptors: a family of hypothalamic neuropeptides and G protein-coupled receptors that regulate feeding behavior. Cell 92, 1 page following 696.

Sakurai, T., Moriguchi, T., Furuya, K., Kajiwara, N., Nakamura, T., Yanagisawa, M., Goto, K., 1999. Structure and function of human prepro-orexin gene. J. Biol. Chem. 274, 17771–17776.

Sasaki, K., Suzuki, M., Mieda, M., Tsujino, N., Roth, B., Sakurai, T., 2011. Pharmacogenetic modulation of orexin neurons alters sleep/wakefulness states in mice. PLoS One 6, e20360.

Szymczak, A.L., Workman, C.J., Wang, Y., Vignali, K.M., Dilioglou, S., Vanin, E.F., Vignali, D.A., 2004. Correction of multi-gene deficiency in vivo using a single 'self-cleaving' 2A peptide-based retroviral vector. Nat. Biotechnol. 22, 589–594.

Thannickal, T.C., Moore, R.Y., Nienhuis, R., Ramanathan, L., Gulyani, S., Aldrich, M., Cornford, M., Siegel, J.M., 2000. Reduced number of hypocretin neurons in human narcolepsy. Neuron 27, 469–474.

Tsujino, N., Yamanaka, A., Ichiki, K., Muraki, Y., Kilduff, T.S., Yagami, K., Takahashi, S., Goto, K., Sakurai, T., 2005. Cholecystokinin activates orexin/hypocretin neurons through the cholecystokinin A receptor. J. Neurosci. 25, 7459–7469.

Tsunematsu, T., Kilduff, T.S., Boyden, E.S., Takahashi, S., Tominaga, M., Yamanaka, A., 2011. Acute optogenetic silencing of orexin/hypocretin neurons induces slow-wave sleep in mice. J. Neurosci. 31, 10529–10539.

Tupone, D., Madden, C.J., Cano, G., Morrison, S.F., 2011. An orexinergic projection from perifornical hypothalamus to raphe pallidus increases rat brown adipose tissue thermogenesis. J. Neurosci. 31, 15944–15955.

Van Den Top, M., Nolan, M.F., Lee, K., Richardson, P.J., Buijs, R.M., Davies, C.H., Spanswick, D., 2003. Orexins induce increased excitability and synchronisation of rat sympathetic preganglionic neurones. J. Physiol. 549, 809–821.

Yamanaka, A., Sakurai, T., Katsumoto, T., Yanagisawa, M., Goto, K., 1999. Chronic intracerebroventricular administration of orexin-A to rats increases food intake in daytime, but has no effect on body weight. Brain Res. 849, 248–252.

Yamanaka, A., Tabuchi, S., Tsunematsu, T., Fukazawa, Y., Tominaga, M., 2010. Orexin directly excites orexin neurons through orexin 2 receptor. J. Neurosci. 30, 12642–12652.

Yi, C.X., Serlie, M.J., Ackermans, M.T., Foppen, E., Buijs, R.M., Sauerwein, H.P., Fliers, E., Kalsbeek, A., 2009. A major role for perifornical orexin neurons in the control of glucose metabolism in rats. Diabetes 58, 1998–2005.